

Supporting Information

Controlled synthesis of Au@AgAu yolk-shell cuboctahedrons with well-defined facets

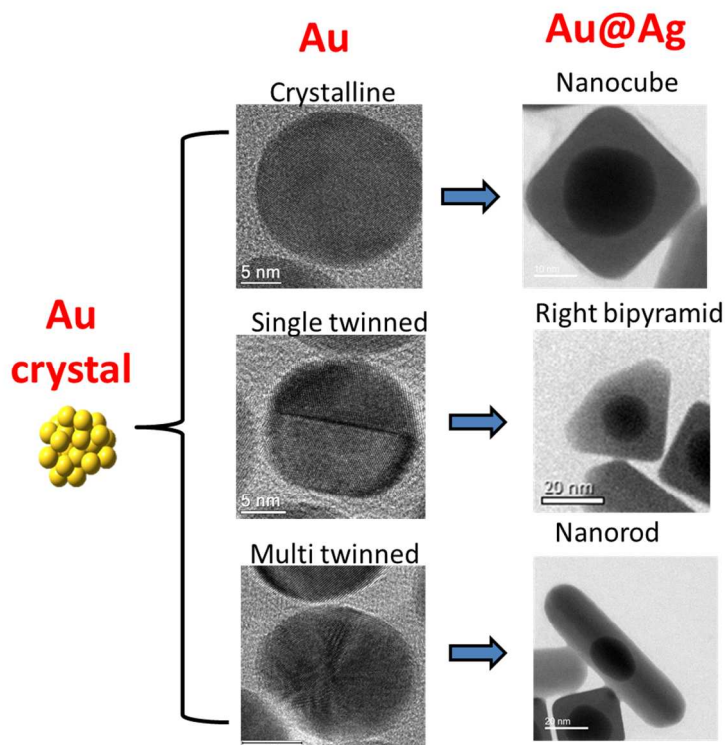
Alejandra Londono-Calderon¹, Daniel Bahena² and Miguel J. Yacaman^{1}*

¹University of Texas at San Antonio, Department of Physics and Astronomy, One UTSA Circle, San Antonio, Texas, 78249, USA.

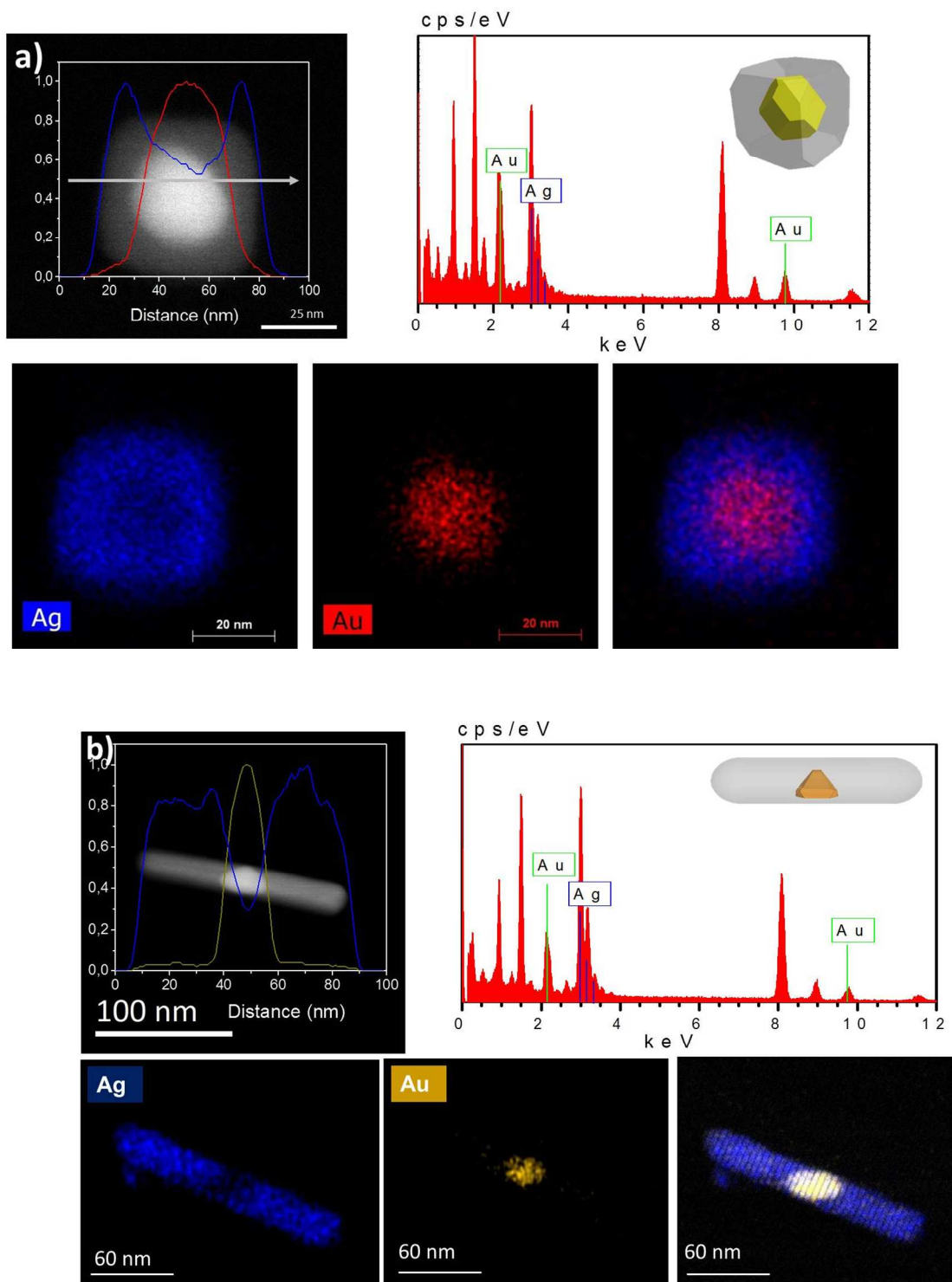
²Advanced Laboratory of Electron Nanoscopy, Cinvestav, Av. Instituto Politecnico Nacional 2508, Col. San Pedro Zacatenco, Delegacion Gustavo A. Madero, Mexico D.F. C.P. 07360, Mexico.

*Corresponding author: miguel.yacaman@utsa.edu

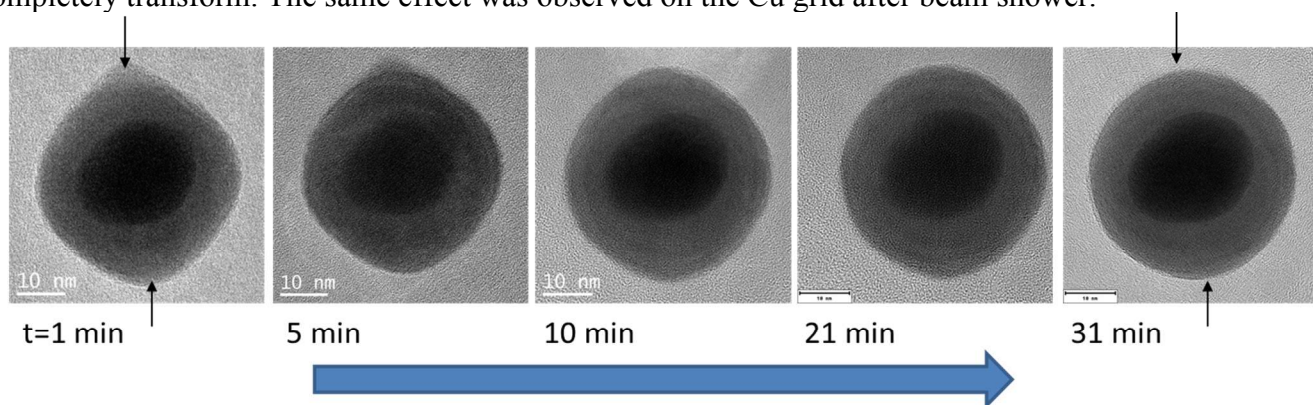
S1. The formation of Au by HAuCl_4 with NaBH_4 leads to the formation of crystalline truncated octahedral, single and, multi twinned Au seeds. The growth of a second metal (Ag) on the surface creates nanocubes, right bipyramids and nanorods depending on the initial Au seed.



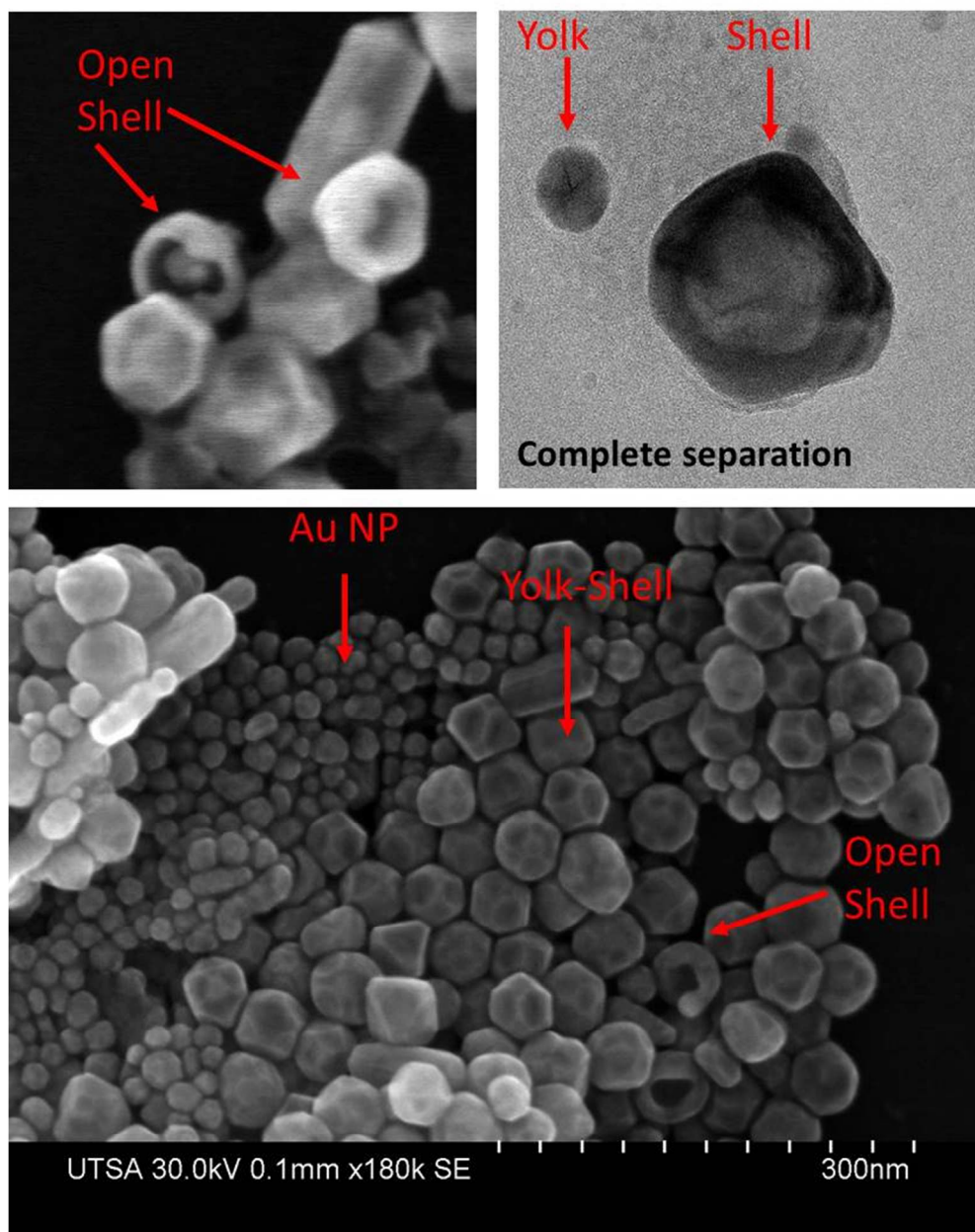
S2. Energy Dispersive X-ray Spectroscopy (EDS) analysis of the Au@Ag core-shell. (a) Line scan and mapping demonstrate the Ag composition of the shell and Au for the core for a nanocube and (b) the same analysis for a core-shell nanorod.



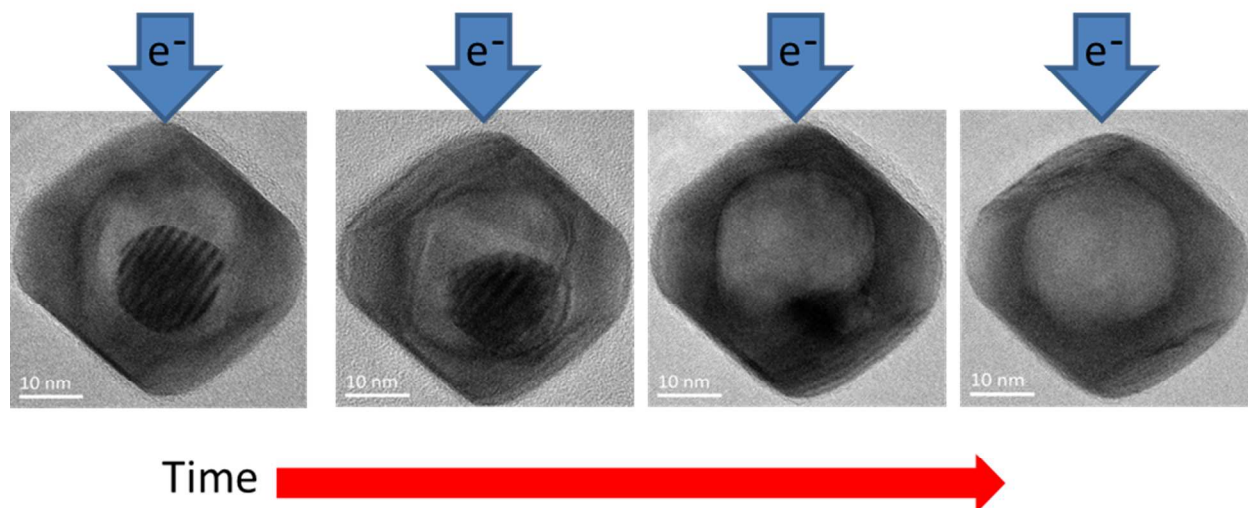
S3. Shape transformation of the silver shell surface due to electron beam interaction. Initially the nanocubes has truncated corner pointed by arrows on the first frame. With the pass of the time the corners started to become rounded. After 31 minutes of the initial frame the particle has completely transform. The same effect was observed on the Cu grid after beam shower.



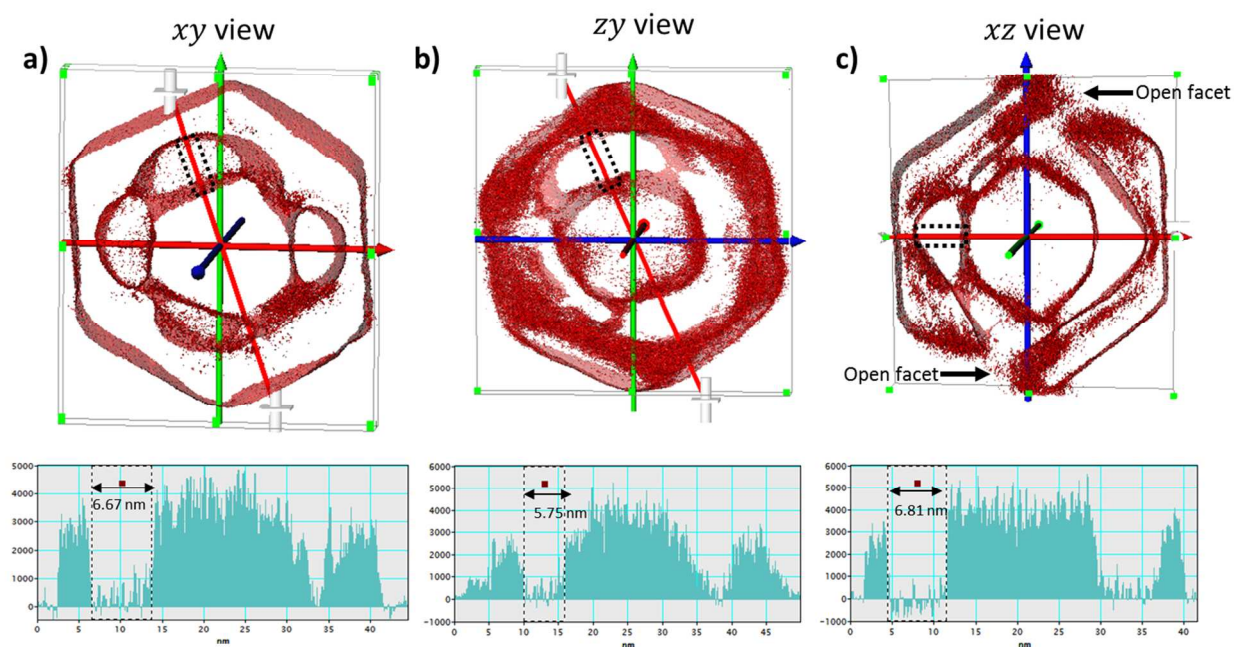
S4. Higher concentration of gold during the third step produce a faster oxidation rate of the silver shell which results on a less homogeneous distribution of particles. When the gold concentration is twice the one reported; cuboctahedrons, octahedrons, and more truncated configurations are obtained besides gold aggregates and open-mouthed yolk shell.



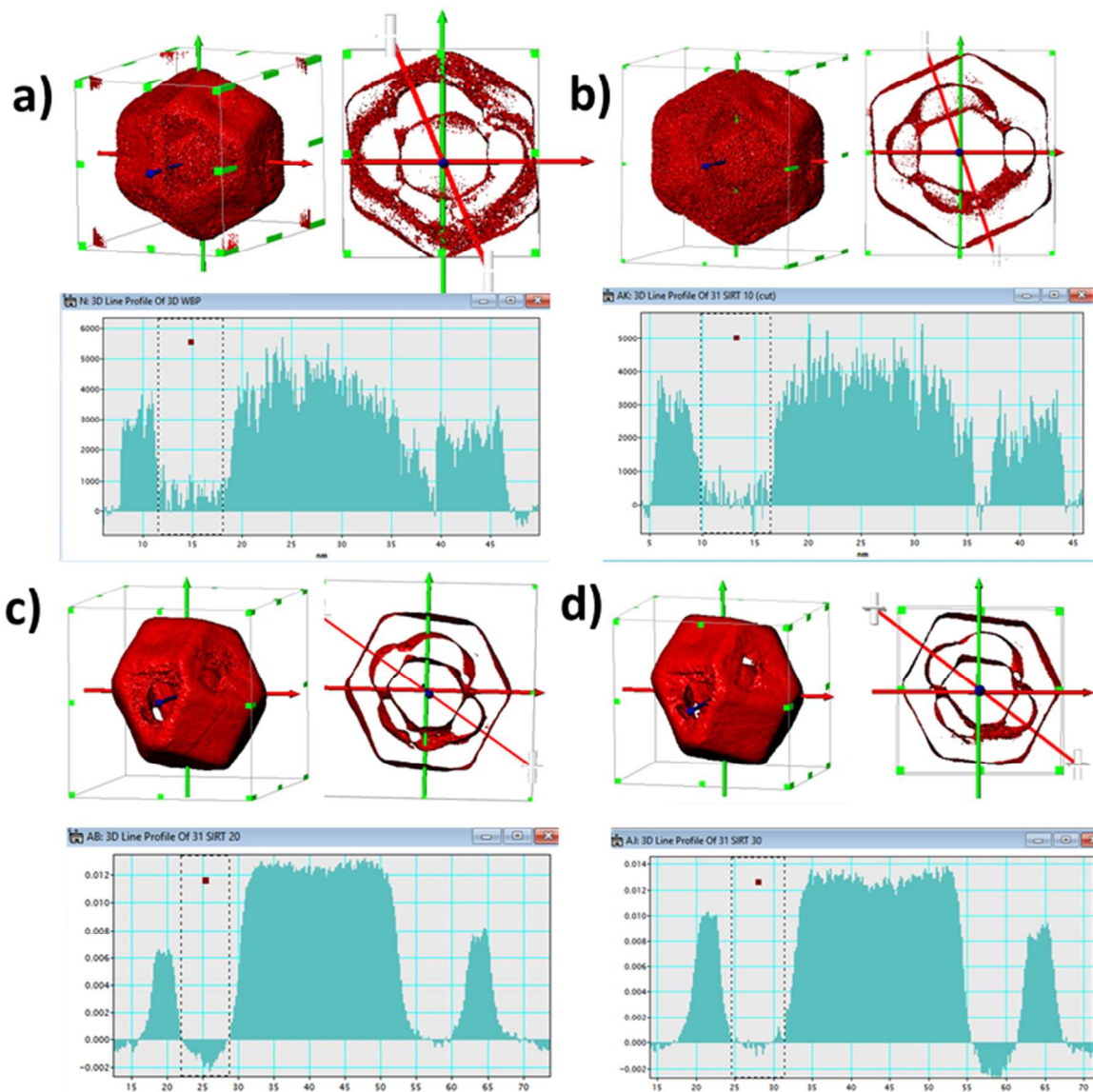
S5. Additional evidence of the diffusion of the Au core on the Au-Ag shell by electron beam interaction.



S6. A thin slice in the center of the reconstructed tomography on three different planes (a) xy , (b) zy and, (c) xz was used to evaluate the size of the inner cavities by a line profile. In general the voids are between 6-7 nm in size. The xz view also allows to observe the discontinuity between planes formed by the open $\{111\}$ facets.



S7. From the same stack of images, using a tilting angle of 31° , different algorithms were used to study the reproducibility of the 3D reconstruction. Each segment shows the same view of the particle, a thin orthoslice on the xy plane and a line profile used to measure the size of the same void by (a) a Weighted Back Projection, Simultaneous Iterative Reconstruction Technique with (b) 10, (c) 20 and, (d) 30 iterations. A table showing the size of the void for each algorithm is also displayed below; the size clearly does not change with the reconstruction technique; the reconstruction shows no differences after 20 iterations. The 3D resolution was determined using Crowther criterion (Ultramicroscopy 111 (2011) 330–336); for a particle of 38 nm in diameter with 125 angular sampling (\sim projections from -62° to $+62^\circ$) the 3D resolution is 1 nm.



	WBP	SIRT 10	SIRT 20	SIRT 30
Size of void (nm)	6.68	6.67	6.56	6.70

This material is available free of charge via the Internet at <http://pubs.acs.org>.